The R factor (0.294) of the MD-refined structure is somewhat higher than the R factor (0.258) of the manually refined structure without solvent and with constant temperature factors; minor model-building is required to correct this difference. The refinement required approximately 1 hour of central processing unit (CPU) time on a CRAY 1; structure factor calculations accounted for about half this time.

As a control, the initial NMR-derived structure was refined without rebuilding by a restrained least-squares method (*2*) that started at 4 Å resolution and then increased the resolution to 3 Å, and finally to 2 Å. The R factor dropped to 0.381, but the very bad stereochemistry and large deviation from the manually refined structure (Table 1) indicated that this structure did not converge to the correct result; residues 34 to 40 did not move (Fig. 1) and substantial model-building would be required to correct the structure. Thus, restrained least-squares refinement in the absence of model-building did not produce the large conformational changes that occurred in MD-refinement.

In another application, MD-refinement was used with human α-lactalbumin, a protein composed of 123 amino acids, for which an initial structure had been obtained by molecular replacement using baboon α-lactalbumin, phasing with the molecular replacement model and preliminary model-building (*14*); conventional refinement had not been done. The initial and the MD-refined structure have R factors of 0.537 and 0.276 at 2.5 Å resolution, respectively; the deviations of bond lengths from ideality of the initial and the MD-refined structure are 0.042 and 0.034 Å, respectively. The rms difference between the initial and MD-refined structure is 1.06 Å and 2.05 Å for backbone and side chain atoms, respectively; eight atoms moved by more than 5 Å during the MD-refinement.

The applicability of the method to a case for which a good initial model is available was examined by using MD-refinement with the α-amylase inhibitor Hoe-467A, a protein composed of 74 amino acids, for which high-resolution x-ray diffraction data and a refined structure exist (*15*); the results are given in Table 1. The initial structure was built from an isomorphous-replacement electron density map and has a relatively low R factor (0.405 at 2.06 Å resolution). MD-refinement was performed at 2.06 Å resolution for 2.5 psec followed by minimization. MD-refinement produced a better R factor than least-squares refinement without model-building (0.271 compared to 0.305, see Table 1) and the same value as manual model-building without solvent and with constant temperature factors.

REFERENCES AND NOTES

1. H. W. Wyckoff, C. H. W. Hirs, S. N. Timasheff, Eds., *Diffraction Methods for Biological Macromolecules, Part B* of *Methods Enzymol.* **115** (1985).
2. W. A. Hendrickson, in (*1*), p. 252; J. H. Konnert and W. A. Hendrickson, *Acta Crystallogr. Sect. A* **36**, 614 (1980).
3. D. S. Moss and A. J. Morffew, *Comput. Chem.* **6**, 1 (1982).
4. J. L. Sussman, S. R. Holbrook, G. M. Church, S. H. Kim, *Acta Crystallogr. Sect. A* **33**, 800 (1977).
5. A. Jack and M. Levitt, *ibid.* **34**, 931 (1978).
6. T. A. Jones, in *Computational Crystallography*, D. Sayre, Ed. (Clarendon, Oxford, 1982), p. 303.
7. S. Kirkpatrick, C. D. Gelatt, Jr., M. P. Vecchi, *Science* **220**, 671 (1983).
8. A. T. Brünger, G. M. Clore, A. M. Gronenborn, M. Karplus, *Proc. Natl. Acad. Sci. U.S.A.* **83**, 3801 (1986).
9. L. Verlet, *Phys. Rev.* **159**, 98 (1967).
10. M. Karplus and J. A. McCammon, *Annu. Rev. Biochem.* **52**, 263 (1983).
11. B. R. Brooks *et al.*, *J. Comput. Chem.* **4**, 187 (1983).
12. W. A. Hendrickson and M. M. Teeter, *Nature (London)* **290**, 107 (1981).
13. A. T. Brünger *et al.*, *Science*, in press.
14. R. E. Fenna, personal communication.
15. J. W. Pflugrath *et al.*, *J. Mol. Biol.* **189**, 383 (1986).

16. We thank M. M. Teeter (*12*) and J. W. Pflugrath (*15*) for providing data, and G. M. Clore, R. E. Fenna, R. Huber, G. A. Petsko, and J. W. Pflugrath for useful discussions. Supported in part by a grant from the National Science Foundation. Computer time on the CRAY 1 and CRAY 2 at the Minnesota Supercomputer Center was supplied by a grant from the Office of Advanced Scientific Computing of the National Science Foundation.

2 September 1986; accepted 26 November 1986

Thunderstorms: An Important Mechanism in the Transport of Air Pollutants

R. R. DICKERSON, G. J. HUFFMAN, W. T. LUKE, L. J. NUNNERMACKER, K. E. PICKERING, A. C. D. LESLIE, C. G. LINDSEY, W. G. N. SLINN, T. J. KELLY, P. H. DAUM, A. C. DELANY, J. P. GREENBERG, P. R. ZIMMERMAN, J. F. BOATMAN, J. D. RAY, D. H. STEDMAN

Acid deposition and photochemical smog are urban air pollution problems, and they remain localized as long as the sulfur, nitrogen, and hydrocarbon pollutants are confined to the lower troposphere (below about 1-kilometer altitude) where they are short-lived. If, however, the contaminants are rapidly transported to the upper troposphere, then their atmospheric residence times grow and their range of influence expands dramatically. Although this vertical transport ameliorates some of the effects of acid rain by diluting atmospheric acids, it exacerbates global tropospheric ozone production by redistributing the necessary nitrogen catalysts. Results of recent computer simulations suggest that thunderstorms are one means of rapid vertical transport. To test this hypothesis, several research aircraft near a midwestern thunderstorm measured carbon monoxide, hydrocarbons, ozone, and reactive nitrogen compounds. Their concentrations were much greater in the outflow region of the storm, up to 11 kilometers in altitude, than in surrounding air. Trace gas measurements can thus be used to track the motion of air in and around a cloud. Thunderstorms may transform local air pollution problems into regional or global atmospheric chemistry problems.

OZONE (O_3) CONTROLS MUCH OF the chemistry of the global atmosphere. When the sun shines on air polluted with automobile exhaust, photochemical reactions of nitrogen dioxide (NO_2), nonmethane hydrocarbons, and carbon monoxide (CO) produce "Los Angeles–type smog" containing high concentrations of O_3 and other oxidants. When these oxidizing agents then react with NO_2 to form nitric acid (HNO_3) and with SO_2 to form sulfuric acid (H_2SO_4), acid rain can result. On a local scale, photochemical smog and acid rain (more accurately called acid deposition) are serious environmental problems; how far these phenomena extend on the regional or global scale is a major unanswered question in atmospheric sciences (*1–3*).

Pollutants travel farther at higher altitudes. In the lowest kilometer of the atmosphere, the planetary boundary layer (PBL), friction with the earth's surface reduces wind speeds. A temperature inversion often isolates the air at the top of the PBL from the rest of the troposphere; the troposphere,

R. R. Dickerson, G. J. Huffman, W. T. Luke, L. J. Nunnermacker, K. E. Pickering, Department of Meteorology, University of Maryland, College Park, MD 20742.
A. C. D. Leslie, C. G. Lindsey, W. G. N. Slinn, Pacific Northwest Laboratory, Richland, WA 99352.
T. J. Kelly and P. H. Daum, Brookhaven National Laboratory, Upton, NY 11973.
A. C. Delany, J. P. Greenberg, P. R. Zimmerman, National Center for Atmospheric Research, Boulder, CO 80307.
J. F. Boatman, National Oceanic and Atmospheric Administration, Boulder, CO 80303.
J. D. Ray and D. H. Stedman, Department of Chemistry, University of Denver, Denver, CO 80210.

extending from the surface to ~14 km, is the layer of the atmosphere where essentially all weather occurs.

The residence times and transport distances of nitrogen and sulfur pollutants are shortest in the PBL. Over North America and Europe, NO_2, NO, and SO_2 are released into the PBL, primarily as a by-product of combustion. Destruction of these compounds occurs predominantly through deposition on the earth's surface, either directly or after oxidation to H_2SO_4 and HNO_3. These sinks are also greatest in the PBL where the relatively warm temperatures, high humidity, and proximity to the earth's surface lead to rapid removal of sulfur and nitrogen compounds. When pollutants are released in or transported to the upper troposphere, the longer lifetimes and higher wind speeds greatly expand their range of influence. Transport of these compounds out of the PBL into the free troposphere (mid- and upper troposphere), however, is generally slow, because the atmosphere is subject to large vertical perturbations only under special circumstances.

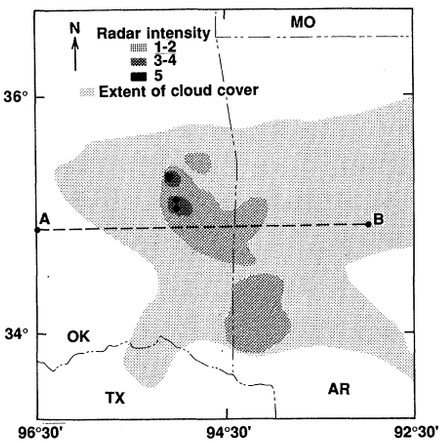

Fig. 1. Meteorological analysis of the research area for 10:00 CST, 15 June 1985. A synthesis of the Oklahoma City, OK, and Monett, MO, radars is superimposed. Level 5 indicates very heavy rain. The outer boundary depicts the horizontal extent of the cloud as indicated by satellite infrared images. One degree of longitude subtends 90 km at 35°N. Line A–B represents the approximate flight track of the research aircraft and depicts the vertical plane along which the thunderstorm was sectioned to produce Fig. 2.

Even at mixing ratios as low as 10 parts per trillion (ppt) by volume, NO and NO_2 efficiently catalyze the photooxidation of nonmethane hydrocarbon (NMHCs) and CO to produce O_3. The lifetimes of nitrogen species are particularly affected by altitude, and efficient transport of PBL air containing NO and NO_2 to the upper troposphere could produce large amounts of O_3 (*3*).

The vertical transport of pollutants is frequently represented mathematically by a process called eddy diffusion (*4*). This can be

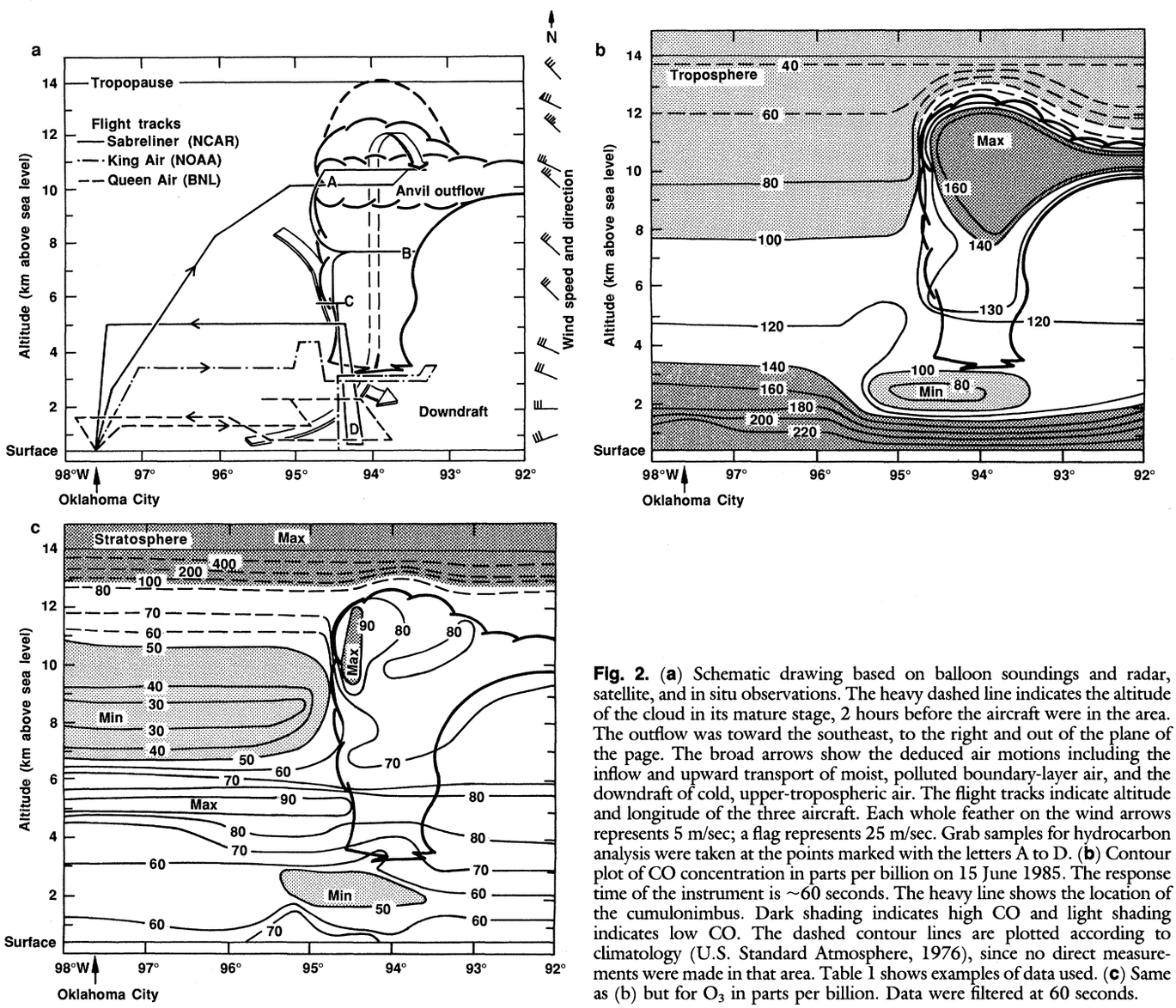

Fig. 2. (**a**) Schematic drawing based on balloon soundings and radar, satellite, and in situ observations. The heavy dashed line indicates the altitude of the cloud in its mature stage, 2 hours before the aircraft were in the area. The outflow was toward the southeast, to the right and out of the plane of the page. The broad arrows show the deduced air motions including the inflow and upward transport of moist, polluted boundary-layer air, and the downdraft of cold, upper-tropospheric air. The flight tracks indicate altitude and longitude of the three aircraft. Each whole feather on the wind arrows represents 5 m/sec; a flag represents 25 m/sec. Grab samples for hydrocarbon analysis were taken at the points marked with the letters A to D. (**b**) Contour plot of CO concentration in parts per billion on 15 June 1985. The response time of the instrument is ~60 seconds. The heavy line shows the location of the cumulonimbus. Dark shading indicates high CO and light shading indicates low CO. The dashed contour lines are plotted according to climatology (U.S. Standard Atmosphere, 1976), since no direct measurements were made in that area. Table 1 shows examples of data used. (**c**) Same as (b) but for O_3 in parts per billion. Data were filtered at 60 seconds.

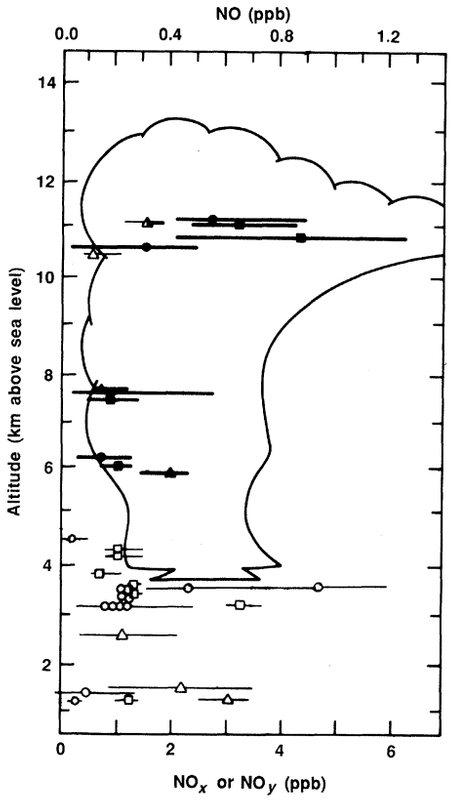

Fig. 3. Reactive nitrogen compounds measured in and around the dissipating thunderstorm. NO, circles; NO_x, squares; and NO_y, triangles; note the different scale for NO. Open symbols show measurements made out of the cloud; filled symbols show measurements made in the cloud; the half-filled symbol shows a measurement made in the transition region as the aircraft exited the cloud. Bars represent the total range. The instrument output was filtered at 10 seconds, and the sampling time for each point was ~150 seconds. See Table 1. Some points are displaced slightly in the vertical for clarity.

Table 1. Data and variability observed on constant altitude legs in and around the thunderstorm; measurements made on ascents and descents are not shown. Aircraft are S, Sabreliner; K, King Air; and Q, Queen Air. Mean ($\bar{x}$), standard deviation (σ), and number of samples (n) are shown for chemical data. Each CO and O_3 sample is a 1.0-minute average; each NO, NO_x, and NO_y sample is a 10-second

Altitude (km)	Aircraft	Temperature (°C)	Dew point (°C)	CO (ppb)			O_3 (ppb)		
				$\bar{x}$	σ	n	$\bar{x}$	σ	n
10.6	S	−48	−53	167	(8)	9	80	(5)	13
10.0	S	−43	≤−55	78	(11)	5	46	(8)	4
10.0	S	−43	−49	173	(5)	2	84	(10)	7
7.6	S	−24	−27	140	(28)	9	70	(5)	16
5.8	S	−11	−13	132	(21)	12	60	(5)	15
5.0	S	−5	−32	124	(8)	16	89	(2)	25
4.5	K	−4	−18				79	(4)	23
3.8	K	4	−6				70	(2)	6
3.1	K	8	0				69	(5)	43
2.6	Q	13	4	70	(14)	21	45	(2)	30
1.7	Q	18	13	190	(10)	30	69	(11)	29
1.1	Q	22	14				60	(2)	8
0.9	S	22	12	214	(10)	14	65	(4)	20

envisioned as a gradual seeping process from regions of high concentration to low. Computer-based models of the atmosphere based on eddy diffusion often use a constant diffusion coefficient, K_z, which corresponds to a few months' time for mixing from the surface to 10 km. NO and NO_2 have chemical lifetimes much shorter than this mixing time, and models using K_z theory predict little or no transport of NO and NO_2 from the PBL to the upper troposphere (*5*).

Deep convection such as occurs during thunderstorms may be an important factor in the chemical composition of the atmosphere (*5*). In a thunderstorm, the transport time for air going from the PBL to 10 km is a matter of hours, not months. Cloud convection as a means of vertical transport is incompletely understood, although it is a key mechanism of circulation within the troposphere. For example, mixing of environmental air into clouds (entrainment) is known to restrict the growth of cumuli, yet knowledge of entrainment dynamics is still limited because suitable tracers of air motion have not been identified (*6*). Fair weather cumulus clouds with tops at 2 to 3 km have been observed to transport air with high concentrations of O_3 out of the PBL (*7*). When unusually high concentrations of pollutants were detected in the free troposphere, deep convection was suggested as the most likely source (*8*). In this report, we present a direct observation of convective transport of photochemically active trace gases in a cumulonimbus, and we paint a portrait of a thunderstorm by means of gas concentrations.

Several research aircraft were outfitted with instruments to measure meteorological parameters and trace gases CO, O_3, NMHCs, and reactive nitrogen compounds NO_x and NO_y. For this experiment, NO_x is defined as the sum of NO, NO_2, and PAN (peroxyacetyl nitrate, an organonitrogen compound characteristic of photochemical smog). NO_y is the sum of NO_x, HNO_3, HO_2NO_2, N_2O_5, and NO_3^-. To reach the outflow region of a thunderstorm (the anvil), a high-flying aircraft is required. For high-altitude work, a Sabreliner—a twin-engine jet operated by the National Center for Atmospheric Research (NCAR)—was used. This aircraft is capable of reaching an altitude of 11 km carrying a full complement of air sensors. For the midtroposphere and PBL, two propeller-driven aircraft—the National Oceanic and Atmospheric Administration (NOAA) King Air and Brookhaven National Laboratory (BNL) Queen Air—were used (*9*).

The flights were conducted in collaboration with the NOAA/NSF (National Science Foundation) PRE-STORM project, which supplied radar and satellite data, balloon soundings, and standard meteorological measurements during May and June 1985.

We selected CO and, to a lesser extent, O_3 as primary tracers of air motion through clouds because they are sparingly soluble in water, rapidly detected, and have atmospheric residence times much longer than the lifetime of a thunderstorm. These gases generally have distinctive tropospheric altitude profiles. CO is produced primarily by ground sources and destroyed throughout the troposphere, and thus generally decreases with altitude. In the clean atmosphere O_3 is produced primarily in the stratosphere and destroyed at the earth's surface, and thus generally increases with altitude. In the polluted atmosphere, photochemical production often generates a local maximum of O_3 in the PBL. Any deviation from environmental profiles of these gases within the cloud during the thunderstorm is presumed to be due to convection.

Like CO, NMHCs are produced at the earth's surface, and any NMHC's found high in the atmosphere have been transported from the earth's surface (*1, 9*). Thus NMHCs, especially the more reactive species, can be used as tracers of atmospheric circulation. Unfortunately, the apparatus for analyzing NMHC is too large to carry on small aircraft; we therefore collected and later measured NMHCs from grab samples taken at discrete points during the flights.

Although only slightly soluble in water, the combination that makes up NO_x is unsuitable as a tracer of air motion because of its high reactivity and because lightning produces NO. The photooxidation of CO and hydrocarbons in the troposphere can either produce or destroy O_3, however, depending on the NO_x catalyst concentration (*3*). If CO and O_3 tracers show convection to be a significant mechanism of transport to the upper troposphere, detection of significant amounts of NO_x in the cloud outflow

average. Instrument noise contributes to the standard deviation of the signal as follows: CO, <6 ppb; O_3, <1 ppb; NO, NO_x, NO_y <0.02 ppb. The temperature and dew point temperature are representative values.

NO (ppb)			NO_x (ppb)			NO_y (ppb)			In or out of cloud
$\bar{x}$	σ	n	$\bar{x}$	σ	n	$\bar{x}$	σ	n	
0.57	(0.13)	14	3.12	(0.74)	13				In
						0.57	(0.18)	11	Out
0.28	(0.15)	13	4.15	(1.40)	15				In
0.18	(0.15)	13	0.91	(0.35)	14	0.88	(0.14)	15	In
0.11	(0.08)	7	0.96	(0.31)	15	2.11	(0.33)	29	In
									Out
0.04	(0.07)	15	1.38	(0.20)	30				Out
			0.78	(0.09)	15				Out
0.17	(0.16)	60	1.18	(0.19)	60				Out
						1.17	(0.28)	184	Out
						2.11	(0.58)	157	Out
0.10	(0.11)	17				2.19	(0.54)	50	Out
0.06	(.01)	13	1.14	(0.17)	30	3.15	(0.20)	28	Out

indicates that convection can be important for O_3 formation in the free troposphere.

The thunderstorm selected for these studies began to develop late on the night of 14 June 1985, when a large mass of cold, dry air moved south over warm moist air from the Gulf of Mexico. The result was an intense band of thunderstorms stretching from Amarillo to Chicago (Fig. 1).

At dawn on 15 June, the aircraft flew toward the expected inflow and outflow regions (Fig. 2a) of a cumulonimbus located near the Oklahoma-Arkansas border. As the Sabreliner climbed in clear air, the mixing ratio of CO fell smoothly (Fig. 2b and Table 1) until the aircraft penetrated the anvil at 10 km. Within seconds the CO level rose sharply. Soon it more than doubled, reaching concentrations rarely observed at this altitude (*1, 10*). The concentration of CO within the cloud was higher than that of CO in the air outside the cloud at all altitudes sampled. The maximim CO level and the core of the outflow appeared to be at about 10 km.

Outside the cloud, O_3 concentrations reached a local maximum of about 99 ppb in a thin layer at about 5 km and a local minimum between 8 and 9 km (Fig. 2c); in the cloud, O_3 reached a maximum of 98 ppb. In the PBL, O_3 was about 65 ppb and CO was about 214 ppb (Table 1), typical of rural continental air and indicative of moderate photochemical smog (*2*).

Four grab samples (Fig. 2a) were taken for NMHC analysis. Table 2 shows representative results. The measurements of NO, NO_x, and NO_y (Fig. 3 and Table 1) indicate fairly uniform concentrations in the PBL, with NO_x comprising about one-third of the NO_y. Concentrations in the cloud outflow region are much higher and much more variable; NO_2 is the dominant NO_y species. At intermediate altitudes in the cloud, ratios of NO_x and NO_y are intermediate between values observed in the PBL and the anvil.

The primary objective of this experiment was to test for polluted PBL air in the outflow region of a thunderstorm. The high levels of CO and NMHCs described prove that the cloud anvil contained air that originated in the lower troposphere and confirm the hypothesis (*5*) that convective processes can be important in the vertical transport of pollutants.

Previous measurements of NO_x and NO_y in the PBL are few, and, as far as we know, there have been no unequivocal measurements of NO_y in the mid- and upper troposphere reported. The levels we observed in the PBL (Fig. 3) were similar to the few previously reported values for rural areas (*2, 9*). At an altitude of 10 km outside the cloud, the measured NO_y value of about 0.6 ppb was in the range of concentrations predicted by computer models (*2, 9*). In the anvil, however, the observed concentrations of NO, NO_x, and NO_y were well above the values expected for the unperturbed upper troposphere (*2, 9*).

Two sources can be identified for the high concentrations of NO_x observed in the cloud. First, NO_x is carried aloft in the updraft of the thunderstorm just as CO and NMHCs are; however, the air in the PBL was not heavily polluted on the day of the thunderstorm, and transport would have contributed a maximum of roughly 1 ppb out of the measured 4 ppb NO_x. Second, lightning produces NO_x (*2*); since this storm generated many cloud-to-ground strokes (*11*), lightning appears to be the principal source of NO_x in the upper cloud.

The wet updraft of the thunderstorm would be expected not only to carry NO_x aloft, but to remove soluble NO_y species such as HNO_3 and NO_3^- from the air as well. The high ratios of NO_x to NO_y observed between 7.6 and 10.6 km support this idea. The injection of fresh NO_x by lightning may also be used to explain these ratios. At least 1 day is required to convert NO_x to other NO_y species.

The downdraft of the thunderstorm (Fig. 2a) can be identified from the trace gas concentrations. There is a local minimum in CO, O_3, reactive nitrogen compounds, and humidity at about 2 km where the vertical air motion in this region was about −1 m/sec (down). At higher altitudes the aircraft apparently flew south of the downdraft. As we expect, the downdraft carries clean, dry air from aloft to the lower troposphere. The apparent origin of the downdraft air at an altitude of 7 to 10 km is higher than was previously observed (*12*). Downdrafts, unlike updrafts, often travel long horizontal distances relative to the size of the cloud, and the possibility that the downdraft originated in the midtroposphere some distance to the northwest of the storm is currently being examined.

The amount of entrainment can be estimated from a comparison of the concentration of CO in the cloud relative to that outside the cloud. If we assume that the anvil was composed of air parcels that started in the PBL and were diluted with upper tropospheric air containing 100 ppb CO, then the anvil was composed of about 64% PBL air and 36% upper tropospheric air. This entrainment is clearly discernible with our chemical tracer technique but is below the detection limit of more conventional thermodynamic tracers (equivalent potential temperature and total water content).

Ozone also reaches a local maximum in the anvil. The O_3 source might have been the layer of high O_3 concentration at 5 km, or, more likely, entrainment of environmental air into the cloud top. When the thunderstorm reached the tropopause (the dividing line between the troposphere and stratosphere) at 14 km, some mixing with O_3-rich, stratospheric air should be expected (*6*). We can approximate the mean entrainment into the cloud top by assuming that the cloud was formed from PBL air containing 65 ppb O_3. If the concentration of O_3 were ~500 ppb at 14 km (Fig. 2c), then an entrainment of 4% would produce the mean O_3 concentration (81 ppb). Electrical corona also produces O_3, but the rate of O_3 production by cloud electrical activity is highly uncertain.

The local O_3 minimum outside the cloud at ~8 km is surprising: ordinarily O_3 increases with altitude in the troposphere. A back trajectory at the 250-mbar level shows that the air had traversed the sparsely populated northwestern United States. In the

Table 2. Observed and calculated nonmethane hydrocarbon concentrations in parts per billion by volume. The uncertainty in these measurements is about 10% for concentrations above 0.1 ppb as carbon. The lifetimes are calculated for the PBL on the basis of O_3 and OH being the only sinks. OH concentrations were taken from Crutzen and Gidel (*10*) and kinetic information from the most recent evaluation by the Jet Propulsion Laboratory (*13*). The upper tropospheric calculations are based on a typical eddy-diffusion rate of mixing, that is, 10 m^2/sec for K_z (*5*).

Hydrocarbon	Lifetime (days)	Mixing ratios (ppb)				
		Observed at			Calculated at	
		PBL	7.6 km	10.6 km	7.6 km	10.6 km
n-Pentane	1.5	0.24	0.16	0.21	1.4×10^{-4}	3.6×10^{-5}
n-Hexane	1.0	7.0×10^{-2}	7.0×10^{-2}	3.0×10^{-3}	6.2×10^{-6}	1.2×10^{-6}
Ethylene	0.6	0.45	0.34	0.11	3.4×10^{-6}	3.0×10^{-7}
Propylene	0.2	0.18	0.12	7.0×10^{-2}	3.4×10^{-11}	4.0×10^{-13}
Benzene	4.8	0.16	0.14	5.0×10^{-2}	2.1×10^{-3}	9.8×10^{-4}
Toluene	0.9	0.14	0.37	2.0×10^{-2}	8.5×10^{-6}	1.5×10^{-6}

very clean troposphere, photochemical processes consume O_3 and CO; if the origin of the air at 8 km were the lower troposphere over the northwestern United States or northern Pacific Ocean (convection was prevalent along the trajectory), then such concentrations are reasonable (*2, 9, 10*).

A second objective of this experiment was to determine whether conventional one-dimensional atmospheric models could adequately predict the concentrations of trace gases that we observed in the upper troposphere. The lifetimes of one class of trace gas, NMHCs, calculated with respect to OH and O_3 attack, vary from several months for slowly reacting compounds such as ethane and acetylene to several hours for faster reacting propylene (*2, 13*). Yet, we observed both long-lived and short-lived NMHCs in the upper troposphere. If the transport time from the surface to the upper troposphere were as long as is assumed in most one-dimensional atmospheric models, the mixing ratios of the short-lived NMHCs would be several orders of magnitude lower than those observed.

Specifically, our NMHC data (Table 2) show that transport models based on slow eddy diffusion cannot adequately explain the mixing ratios of the short-lived NMHCs measured at 7.6 and 10.6 km. The one-dimensional model we tested uses the standard eddy-diffusion transport scaled to describe average vertical transport in the troposphere and includes the major chemical loss mechanisms for hydrocarbons, that is, OH and O_3 attack. It is based on the same principles as many models described in the literature (*5*).

Our results support the hypothesis that anthropogenic emissions of NO_x and NMHC, which react in the presence of sunlight to form O_3, can increase tropospheric O_3 on a large scale. Such an increase would have a major impact on global tropospheric chemistry and aggravate the global warming from other atmospheric trace gases such as CO_2 (*2*). On the other hand, the same convective process that transports NO_x and NMHCs to the upper troposphere may also transport and dilute anthropogenic NO_x and SO_2, lessening the amount of man-made acid deposited locally. We therefore suggest that convective processes must be considered in models of tropospheric photochemistry and acid deposition.

The storm used in our study was too large to circumnavigate. By selecting smaller, single-celled storms and flying closed patterns at numerous altitudes around the cloud, researchers will be able to construct a three-dimensional, chemical, and dynamic picture of the cloud environment. The updraft of a deep cloud is dangerous to enter because of icing and hail. Smaller clouds, especially at altitudes above or well below the freezing level, can be penetrated safely. Ideally, a high-flying airplane with deicing capabilities could be used in conjunction with current radar information.

Cloud physicists have expended considerable effort in investigating the exchange of air between clouds and the air that surrounds them (entrainment or detrainment). Most of these investigations have used thermodynamic techniques to quantify the amount and sources of entrainment (*6*). The thermodynamic techniques require the measurement of temperature, pressure, and water content (both liquid and vapor) in and near the clouds. The comparatively small difference in thermodynamic properties between a cloud and the surrounding air dictates that the thermodynamic variables be measured very accurately. We suggest that trace gases can provide a useful tool for visualizing entrainment in convective systems, and will prove to be increasingly useful in future studies of cloud dynamics.

REFERENCES AND NOTES

1. *Acid Deposition: Atmospheric Processes in Eastern North America* (National Academy Press, Washington, DC, 1983); *Global Tropospheric Chemistry, A Plan for Action* (National Academy Press, Washington, DC, 1984).
2. D. Kley, J. W. Drummond, M. McFarland, S. C. Liu, *J. Geophys. Res.* **86**, 3153 (1981); J. A. Logan, *ibid.* **88**, 10785 (1983); D. H. Stedman and R. E. Shetter, in *Trace Atmospheric Constituents: Properties, Transformations and Fates* (Wiley, New York, 1983), pp. 411–454; R. E. Dickinson and R. J. Cicerone, *Nature (London)* **319**, 109 (1986); J. A. Logan, *J. Geophys. Res.* **90**, 10463 (1985).
3. W. Chameides and J. C. G. Walker, *J. Geophys. Res.* **78**, 8751 (1973); P. J. Crutzen, *Pure Appl. Geophys.* **106**, 1385 (1973); J. Fishman and P. J. Crutzen, *Nature (London)* **274**, 855 (1978).
4. Conventionally, properties of the atmosphere such as the vertical velocity (W) are represented as $W = \overline{W} + W'$, where the bar represents the "Reynolds average" and the prime, the deviation from the mean. If the statistics of the fluctuations do not change rapidly with time, the time-averaged deviations vanish so the mean upward flux of some trace gas is $\overline{F} = \overline{WC} + \overline{W'C'}$, where C is the concentration of the trace gas. The long-term average vertical air motion ($\overline{W}$) must be zero on level terrain, so vertical mixing in the atmosphere can occur only by eddy diffusion—a continuous, slow process. The exact representation of the $\overline{W'C'}$ term is an important and unsolved problem in turbulence. One popular approximation is K_z theory, in which $\overline{W'C'}$ is represented by
$$\overline{W'C'} = \frac{d}{dz}\left(K_z \frac{dC}{dz}\right)$$
where K_z is the eddy-diffusion coefficient in the vertical (z) direction. See, for example, J. Holton, *An Introduction to Dynamic Meteorology* (Academic Press, New York, 1979).
5. R. B. Chatfield, thesis, Colorado State University (1982); L. T. Gidel, *J. Geophys. Res.* **88**, 6587 (1983); J. A. Ritter, thesis, University of Michigan (1983); R. B. Chatfield and P. J. Crutzen, *J. Geophys. Res.* **89**, 7111 (1984).
6. For a current review of cumulus entrainment studies, see G. W. Reuter, *Bull. Am. Meteorol. Soc.* **67**, 151 (1986).
7. G. K. Greenhut, J. K. S. Ching, R. Pearson, Jr., T. P. Repoff, *J. Geophys. Res.* **89**, 4757 (1984); G. K. Greenhut, *ibid.* **91**, 8613 (1986).
8. S. T. Shipley *et al.*, *Environ. Sci. Technol.* **18**, 749 (1983); D. Ehhalt, J. Rudolph, F. Meixner, V. Schmidt, *J. Atmos. Chem.* **3**, 29 (1985); R. J. Ferek, R. B. Chatfield, M. O. Andreae, *Nature (London)* **320**, 514 (1986).
9. Analytical techniques and earlier measurements are described in the following: R. L. Tanner, P. H. Daum, T. J. Kelly, *Int. J. Environ. Anal. Chem.* **13**, 323 (1983); R. R. Dickerson, A. C. Delany, A. F. Wartburg, *Rev. Sci. Instrum.* **55**, 1995 (1984); R. R. Dickerson, *Atmos. Environ.* **18**, 2585 (1984); J. Greenberg and P. R. Zimmerman, *J. Geophys. Res.* **89**, 4767 (1984); T. Kelly, R. Tanner, L. Newman, P. J. Galvin, J. A. Kadlecek, *Atmos. Environ.* **18**, 2565 (1984); B. S. Gockel, R. R. Dickerson, G. J. Huffman, paper presented at the 27th Rocky Mountain Conference, Rocky Mountain Section of the Society for Applied Spectroscopy and Rocky Mountain Chromatography Discussion Group, Denver, Colorado, 14 to 18 July 1985.
10. P. J. Crutzen and L. T. Gidel, *J. Geophys. Res.* **88**, 6641 (1983); J. Fishman and W. Seiler, *ibid.*, p. 3662; M. A. K. Khalil and R. A. Rasmussen, *Science* **224**, 54 (1984).

11. J. G. Meitín and J. B. Cunning, *NOAA Tech. Memo ERL ESG-20* (National Oceanic and Atmospheric Administration, Boulder, CO, 1985).
12. R. A. Houze, *Mon. Weather Rev.* **105**, 1540 (1977), E. J. Zipser, *ibid.*, p. 1568.
13. NASA, "Chemical kinetics and photochemical data for use in stratospheric modeling" (Publ. 85-37, Jet Propulsion Laboratory, Pasadena, CA, 1985).
14. We thank D. Apple, R. Brown, J. Cunning, S. Fink, B. Gockel, L. Gunter, D. Kita, P. Klotz, D. Leahy, J. Meitin, D. Rodenhuis, D. Wellman, and L. Wolpert who contributed to the success of the project. We also thank the Research Aviation Facility staff of NCAR, notably, R. Burris, E. Miller, and J. Ragni; . A. Schanot was especially helpful. Discussions with R. Chatfield, P. Crutzen, and E. Zipser were enlightening. This report was taken from a dissertation to be submitted to the Graduate School, University of Maryland, by W.T.L. in partial fulfillment of the requirements for the Ph.D. degree in chemistry. This work was conducted under the joint sponsorship of NSF (grant ATM-83-05843 and PRE-STORM), Department of Energy (PRECP), and NOAA (PRE-STORM). NCAR is sponsored by NSF.

14 July 1986; accepted 31 October 1986

Validity Tests of the Mixing-Length Theory of Deep Convection

KWING L. CHAN AND SABATINO SOFIA

The construction of solar or stellar models is hindered by the difficulty of computing, with sufficient accuracy, the convective fluxes in unstable regions. Although the mixing-length theory of convection has been used for more than three decades, its validity has neither been tested by experiment nor verified by computation. This report presents the results of a three-dimensional numerical simulation of deep and efficient convection that support two conclusions: (i) the basic picture proposed by the mixing-length theory is physically valid—the vertical correlation of the motion of fluid elements is proportional to the pressure scale height; and (ii) some dynamical variables, including the convective flux, can be approximately computed from the structure of the stratification with mixing-length approximations.

THE MIXING-LENGTH THEORY (MLT) of convection (*1, 2*) is at present the only practical approach for calculating convective fluxes in highly stratified convection zones. MLT is widely applied in many areas of astrophysical and geophysical fluid dynamics (*3, 4, 5*); in particular, a major part of solar and stellar theory depends on its validity. Despite this extensive use, the validity of MLT has remained controversial because it drastically simplifies the complex phenomenon of turbulent flow in a stratified compressible medium (*6*). Like any approximation, MLT will be inadequate to describe some features of the flow but possibly adequate for describing others. Thus, it would be useful to establish the domain of validity for the theory. Whereas many studies (for example, simulation of the solar granules or computation of the pulsation-convection coupling) require detailed dynamical information that cannot be provided by MLT, other studies, such as stellar evolution, depend primarily on global flux information. A likely area of success for MLT is therefore the flux computation. We report results of numerical simulations that support the validity of two key elements of MLT, namely, the mixing-length concept itself, and the determination of the local dynamical variables that are essential to the flux calculation.

The average heat (enthalpy) flux, F, carried by the convective motions in an efficiently convecting layer is given by

$$F = \rho C_p C(V_z,\Delta T)V'T' \qquad (1)$$

where ρ is the density, C_p is the specific heat for constant pressure, and $C(V_z,\Delta T)$ is the correlation between the vertical velocity V_z and the temperature fluctuation ΔT, whose root-mean-square values are V' and T', respectively. MLT assumes that the convective heat transfer is performed by "bubbles" associated with temperature fluctuations. After traveling a characteristic distance, the mixing length ℓ, the bubbles "dissolve" back into the environment, so that V' and T' can be determined as (*7*)

$$V' \simeq (gH\Delta\nabla)^{1/2}\,(\ell/H) \qquad (2)$$

$$T' \simeq T\Delta\nabla(\ell/H) \qquad (3)$$

where g is the gravitational acceleration, H is the pressure scale height,

$$\Delta\nabla = \frac{\partial \ln(T)}{\partial \ln(p)} - \left[\frac{\partial \ln(T)}{\partial \ln(p)}\right]_{ad} \qquad (4)$$

is the superadiabatic gradient, which is a measure of how far the stratification is away from static stability, and p is the pressure. Note that the symbol $\simeq$ in the above equations absorbs factors of order unity which would not alter the fundamental scaling relations. The choice of ℓ is a serious uncertainty of MLT. The usual assumption is that $\ell = \alpha H$, where α, the mixing-length ratio, is a constant of order unity; however, some investigators prefer to use the density scale height instead of H as the scale length (*8, 9*).

To assess the validity of the mixing-length theory and its assumptions, we solve the Navier Stokes equations for an ideal compressible gas to simulate deep and efficient convection. The domain of computation is a rectangular box having width 1.5 times the depth. The sides have periodic boundary conditions, and the top and bottom are impenetrable and stress-free. A constant energy flux is supplied at the bottom, and the value of entropy is fixed at the top. The initial distribution is polytropic (the temperature gradient is uniform, and the density is a power function of the temperature) and slightly superadiabatic. For the computation, we use units that make the density, pressure, and temperature at the top, and the total depth, all equal to 1. The initial state is perturbed by a weak velocity field in the form of a few regular cells. An implicit

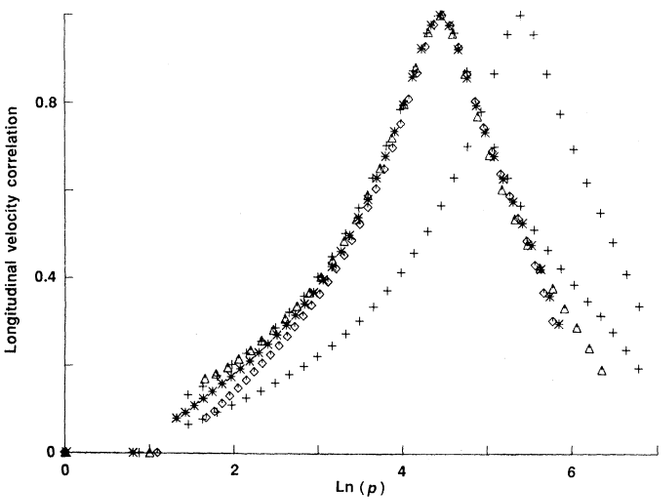

Fig. 1. Longitudinal correlation A of vertical velocities plotted against the logarithmic pressure $\ln p$ for the different numerical cases. (+) case a; (*) case b; (◇) case c; (△) case d, which has a different value of γ from the other three cases.

K. L. Chan, Applied Research Corporation, Landover, MD 20785.
S. Sofia, Center for Solar and Space Research, Yale University, New Haven, CT 06511.